

A Combined Numerical and Analytical Approach for Magnetic Field Analysis of Permanent Magnet Machines

Z. J. Liu, C. Bi, H. C. Tan and T-S. Low
Magnetics Technology Centre, National University of Singapore, Singapore 0511

Abstract—This paper discusses finite element analysis of permanent magnet machines using an annular macro-element for the air gap and magnet region. It is shown that in comparison with the conventional finite element scheme, the proposed method provides stable computational prediction of magnetic field problem, and can be used as design and analysis tool for permanent magnet machines.

I. INTRODUCTION

One of the problems with applying the finite element method (FEM) to design and analysis of electrical machines is that the computational results are sensitive to the mesh arrangement and the local density of node distribution. In analysis of magnetic field problems in permanent magnet (PM) electric machine, for example, a high level of mesh density in the air gap region and the magnet region is necessary to achieve reliable predictions, since most of the energy in the machine is stored in those regions. Furthermore, an accurate calculation of the magnetic field distribution in electrical machines is essential for torque and force predictions.

The application of "air-gap element", or otherwise known as "macro-element"[1], to the finite element analysis of electrical machines was first discussed in references [1,2]. The major advantage of the idea is that the sensitivity of the finite element solution to the mesh in the air gap region can be eliminated. Numerical techniques based on this idea are seen to be effective to achieve higher accuracy in air gap field prediction, particularly when dynamic analysis of electrical machines is in question.

This paper introduces an annular macro-element (M.E) that involves machine air gap and magnet region, i.e. an "active" M.E. that contains field excitation sources, for magnetic field computation of permanent magnet machines with internal rotor having surface-mounted magnet poles. An analytical expression for the magnetic field, described vector potentials, in the M.E. region will be developed to describe the relationship between the node potentials, A_i , at the M.E. boundary and the field excitation sources due to the magnet poles. The finite element formulation for the M.E. and the slotted stator laminations having non-linear magnetic characteristics is also described in the paper. The proposed method will be then applied to magnetic field analysis of a PM dc motor which has surface-mounted NdFeB magnet poles. A comparison is made between the theoretical prediction of the field problem obtained from the proposed method and those obtained from the conventional FEM. It is shown that the proposed method can

provide stable computational predictions of magnetic field problem, and can be used as design and analysis tool for permanent magnet machines.

II. ANALYTICAL SOLUTIONS OF MAGNETIC FIELD PROBLEM IN MACRO-ELEMENT

The cross-section view of a PM electrical machine with internal rotor topology is shown in Fig. 1. The region for the slotted stator laminations is discretized with finite element mesh. This section presents an analytical expression for the field problem in a M. E. that is formed by the regions of air gap, magnet and the rotor back iron. The solution is useful since the level of saturation is usually low in the rotor back iron for this type of machine.

The total region of the M.E., Ω_{me} , is divided into three sub-regions, as illustrated in Fig. 1. Using vector potential, \bar{A}_i , which satisfies the relation $\nabla \times \bar{A} = \bar{B}$, the general form of the governing equation can be expressed as follows:
REGION 1: (air gap)

$$\frac{\partial^2 A_1}{\partial r^2} + \frac{1}{r} \frac{\partial A_1}{\partial r} + \frac{1}{r^2} \frac{\partial^2 A_1}{\partial \theta^2} = 0 \quad (1)$$

REGION 2 (magnets with interloper gaps)

$$\frac{\partial^2 A_2}{\partial r^2} + \frac{1}{r} \frac{\partial A_2}{\partial r} + \frac{1}{r^2} \frac{\partial^2 A_2}{\partial \theta^2} = \frac{1}{r} \frac{\partial M(\theta)}{\partial \theta} \quad (2)$$

REGION 3: (rotor back iron)

$$\frac{\partial^2 A_3}{\partial r^2} + \frac{1}{r} \frac{\partial A_3}{\partial r} + \frac{1}{r^2} \frac{\partial^2 A_3}{\partial \theta^2} = 0 \quad (3)$$

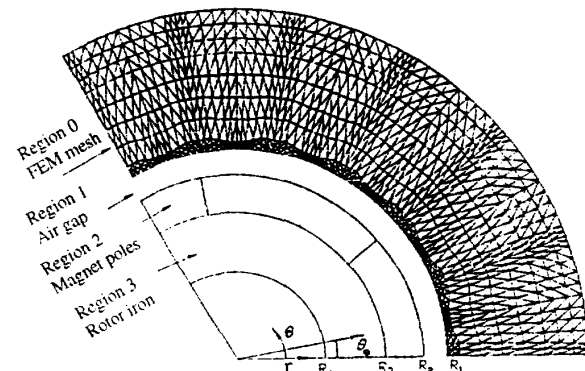


Fig. 1 Cross-section view of a PM motor, showing the macro-element and finite element mesh for slotted stator laminations

In the above equations, $M(\theta)$ is the magnetization of magnets, which can be expressed as follows:

$$M(\theta) = \sum_{N=1}^{\infty} \frac{4B_r}{\pi N} \sin(N\pi\tau_p/2) \cos Np(\theta - \theta_0)$$

where $N = 1, 3, 5, \dots$, B_r is the remanence of magnets, p is the number of pole pairs, τ_p is the ratio of pole arc over pole pitch, and θ_0 is the angle between the reference axis for the magnet poles and the reference polar coordinate frame for the machine stator, as shown in Fig. 1.

The general solution to the equations (1) - (3) can be found as:

$$A_k(r, \theta) = \sum_N \left\{ \left[A_{kN} r^n + B_{kN} r^{-n} + \frac{a_{kN} \sin n\theta_0}{1-n^2} nr \right] \cos n\theta + \left[C_{kN} r^n + D_{kN} r^{-n} - \frac{a_{kN} \cos n\theta_0}{1-n^2} nr \right] \sin n\theta \right\} + (A'_{k0} \ln r + B'_{k0})(C'_{k0} \theta + D'_{k0}) \quad (4)$$

where $k = 1, 2, 3$, $N = 1, 2, 3, \dots$, $n = Np$, and

$$a_{kN} = \begin{cases} \frac{4M_r \sin(N\pi\tau_p/2)}{\pi N} & \text{if } k=2 \text{ and } N=1, 3, 5, \dots \\ 0 & \text{otherwise} \end{cases} \quad (5)$$

In Equ. (4), $A_{kN}, B_{kN}, C_{kN}, D_{kN}, A'_{k0}, B'_{k0}, C'_{k0}$, and D'_{k0} are arbitrary constants to be determined by boundary conditions, which for the studied field problem can be defined as follows:

$$A_1|_{r=R_1} = \sum_N [\Psi_N \cos n\theta + \Phi_N \sin n\theta] \quad (6)$$

$$A_2|_{r=R_2} = A_1|_{r=R_2} \quad (7)$$

$$\frac{1}{\mu_2} \frac{\partial A_2}{\partial r} \Big|_{r=R_2} = \frac{1}{\mu_1} \frac{\partial A_1}{\partial r} \Big|_{r=R_2} \quad (8)$$

$$A_3|_{r=R_3} = A_2|_{r=R_3} \quad (9)$$

$$\frac{1}{\mu_3} \frac{\partial A_3}{\partial r} \Big|_{r=R_3} = \frac{1}{\mu_2} \frac{\partial A_2}{\partial r} \Big|_{r=R_3} \quad (10)$$

$$\frac{\partial A_3}{\partial \theta} \Big|_{r=R_4} = 0 \quad (11)$$

In boundary condition (6), Ψ_N and Φ_N are derived from the vector potential distribution A_i on nodes $r = R_1$ and $\theta = \theta_i$ ($i = 1, 2, \dots, m$). Therefore Ψ_N and Φ_N can be described by:

$$\begin{aligned} \Psi_N &= \sum_{i=1}^m \zeta_{Ni} A_i \\ \Phi_N &= \sum_{i=1}^m \xi_{Ni} A_i \end{aligned} \quad (12)$$

where ζ_{Ni} and ξ_{Ni} are the Fourier coefficients obtained from the Fourier expansion of A_i at boundary $r = R_i$.

$$\zeta_{Ni} = \begin{cases} \frac{2}{\pi N^2 p (\theta_1 - \theta_2)} \sin \frac{n}{2} (\theta_2 + \theta_1) \sin \frac{n}{2} (\theta_1 - \theta_2) & i = 1 \\ \frac{(-2)}{\pi N^2 p (\theta_m - \theta_{m-1})} \sin \frac{n}{2} (\theta_m + \theta_{m-1}) \sin \frac{n}{2} (\theta_m - \theta_{m-1}) & i = m \\ \frac{1}{\pi N^2 p} \left[\frac{\cos n\theta_i - \cos n\theta_{i-1}}{(\theta_i - \theta_{i-1})} + \frac{\cos n\theta_i - \cos n\theta_{i+1}}{(\theta_i - \theta_{i+1})} \right] & \end{cases} \quad (13)$$

$$\xi_{Ni} = \begin{cases} \frac{(-2)}{\pi N^2 p (\theta_1 - \theta_2)} \cos \frac{n}{2} (\theta_2 + \theta_1) \sin \frac{n}{2} (\theta_1 - \theta_2) & i = 1 \\ \frac{2}{\pi N^2 p (\theta_m - \theta_{m-1})} \cos \frac{n}{2} (\theta_m + \theta_{m-1}) \sin \frac{n}{2} (\theta_m - \theta_{m-1}) & i = m \\ \frac{1}{\pi N^2 p} \left[\frac{\cos n\theta_i - \cos n\theta_{i-1}}{(\theta_i - \theta_{i-1})} + \frac{\cos n\theta_i - \cos n\theta_{i+1}}{(\theta_i - \theta_{i+1})} \right] & \end{cases} \quad (14)$$

Applying boundary conditions (6) - (11) to the general solution (4), we have the expression of the vector potential distribution in the sub regions as below

$$A_k = \sum_{i=1}^m v_{ki} A_i + \sum_{N=1}^{\infty} \frac{a_{kN}}{Q_N (1-n^2)} [f_{kN} r^n + g_{kN} r^{-n} + Q_N r] \cos n(\theta - \theta_0) \quad (15)$$

where

$$v_{ki} = \frac{1}{2} \frac{\ln r}{\ln R_1 / R_4} \zeta_{0i} + \sum_N \frac{1}{Q_N} (a_{kN} r^n + \beta_{kN} r^{-n}) (\zeta_{Ni} \cos n\theta + \xi_{Ni} \sin n\theta) \quad (16)$$

in above two equations

$$Q_N = (S_N + T_N) R_1^n$$

$$S_N = \lambda_1 \left[\gamma_1 - \gamma_2 \left(\frac{R_4}{R_3} \right)^{2n} \right] + \lambda_2 \left[\gamma_2 - \gamma_1 \left(\frac{R_4}{R_3} \right)^{2n} \right] \left(\frac{R_3}{R_2} \right)^{2n}$$

$$T_N = \left\{ \lambda_2 \left[\gamma_1 - \gamma_2 \left(\frac{R_4}{R_3} \right)^{2n} \right] + \lambda_1 \left[\gamma_2 - \gamma_1 \left(\frac{R_4}{R_3} \right)^{2n} \right] \right\} \left(\frac{R_3}{R_2} \right)^{2n} \left(\frac{R_2}{R_1} \right)^{2n}$$

$$\lambda_1 = 1 + \frac{\mu_1}{\mu_2}, \quad \lambda_2 = 1 - \frac{\mu_1}{\mu_2}, \quad \gamma_1 = 1 + \frac{\mu_2}{\mu_3}, \quad \text{and} \quad \gamma_2 = 1 - \frac{\mu_2}{\mu_3}$$

$$\alpha_{1N} = S_N, \quad \beta_{1N} = T_N R_1^{2n}, \quad g_{1N} = f_{1N} R_1^{2n}$$

$$f_{1N} = \frac{\mu_1}{\mu_2} \left[2 \left[n \frac{\mu_2}{\mu_3} \left(1 + \left(\frac{R_4}{R_3} \right)^{2n} \right) - \left(1 - \left(\frac{R_4}{R_3} \right)^{2n} \right) \right] \left(\frac{R_3}{R_1} \right)^n R_3 \right. \\ \left. - \left[\gamma_1 - \gamma_2 \left(\frac{R_4}{R_3} \right)^{2n} \right] \left[(n-1) \left(\frac{R_2}{R_1} \right)^n R_2 + \left[\gamma_2 - \gamma_1 \left(\frac{R_4}{R_3} \right)^{2n} \right] (n+1) \left(\frac{R_3}{R_2} \right)^n \left(\frac{R_3}{R_2} \right)^n R_2 \right] \right]$$

$$\alpha_{2N} = 2 \left[\gamma_1 - \gamma_2 \left(\frac{R_4}{R_3} \right)^{2n} \right], \quad \beta_{2N} = 2 \left[\gamma_2 - \gamma_1 \left(\frac{R_4}{R_3} \right)^{2n} \right] R_3^{2n}$$

$$f_{2N} = \left[n \frac{\mu_2}{\mu_3} \left(1 + \left(\frac{R_4}{R_3} \right)^{2n} \right) - \left(1 - \left(\frac{R_4}{R_3} \right)^{2n} \right) \right] \left[\lambda_1 \left(\frac{R_3}{R_1} \right)^n + \lambda_2 \left(\frac{R_3}{R_2} \right)^n \left(\frac{R_1}{R_2} \right)^n \right] R_3 \\ - \left[\gamma_1 - \gamma_2 \left(\frac{R_4}{R_3} \right)^{2n} \right] \left[\left(n + \frac{\mu_1}{\mu_2} \right) \left(\frac{R_1}{R_2} \right)^n + \left(n - \frac{\mu_1}{\mu_2} \right) \left(\frac{R_2}{R_1} \right)^n \right] R_2$$

$$g_{2N} = \left[\left(1 - \left(\frac{R_4}{R_3} \right)^{2n} \right) - n \frac{\mu_2}{\mu_3} \left(1 + \left(\frac{R_4}{R_3} \right)^{2n} \right) \right] \left[\lambda_1 \left(\frac{R_1}{R_3} \right)^n + \lambda_2 \left(\frac{R_2}{R_1} \right)^n \left(\frac{R_2}{R_3} \right)^n \right] R_3^{2n} R_3 \\ + \left[\gamma_2 - \gamma_1 \left(\frac{R_4}{R_3} \right)^{2n} \right] \left[\left(n + \frac{\mu_1}{\mu_2} \right) \left(\frac{R_1}{R_2} \right)^n + \left(n - \frac{\mu_1}{\mu_2} \right) \left(\frac{R_2}{R_1} \right)^n \right] R_3^{2n} R_2$$

$$f_{3N} = \left[\lambda_1 (n+1) \left(\frac{R_1}{R_3} \right)^n R_3 + \lambda_2 (n-1) \left(\frac{R_3}{R_2} \right)^n \left(\frac{R_1}{R_2} \right)^n R_3 - 2 \left(n + \frac{\mu_1}{\mu_2} \right) \left(\frac{R_1}{R_2} \right)^n R_2 \right] + \\ + \left[\lambda_2 (n+1) \left(\frac{R_2}{R_3} \right)^n \left(\frac{R_2}{R_1} \right)^n R_3 + \lambda_1 (n-1) \left(\frac{R_3}{R_1} \right)^n R_3 - 2 \left(n - \frac{\mu_1}{\mu_2} \right) \left(\frac{R_2}{R_1} \right)^n R_2 \right]$$

$$\alpha_{3N} = 4, \quad \beta_{3N} = -4 R_4^{2n}, \quad g_{3N} = -f_{3N} R_4^{2n}.$$

III. FINITE ELEMENT FORMULATION OF MACRO ELEMENT

The rest of the machine, as shown in Fig. 1, is discretized by the triangular finite element mesh. The finite element formulation of these elements, Ω_e , for magnetic field problems can be established to obtain the equations in the form of:

$$[S_{ij}]_e [A_i]_e - [q_i]_e = 0$$

where $[S_{ij}]$ and $[q_i]$ represent the stiff matrix and the column vector of field source term in an element.

Obviously, one way of combining the finite element solution for the non-linear region of the stator laminations and the analytical solution for the region M.E. is to use an iterative procedure. However, such an iteration approach requires long computing time for the solution of the overall magnetic field problem to converge. In this paper the Galerkin method, which can be stated as:

$$\int_{\Omega_{ME}} \frac{1}{\mu_e} \left(\frac{\partial w_k}{\partial r} \frac{\partial A_k}{\partial r} + \frac{1}{r} \frac{\partial w_k}{\partial \theta} \frac{1}{r} \frac{\partial A_k}{\partial \theta} - w_k J_{ME} \right) d\Omega - \oint_{\Gamma} \frac{1}{\mu_e} w_j \frac{\partial A_k}{\partial n} d\Gamma = 0 \quad (17)$$

is used, with A_k as the unknowns and $w_k = \sum_i^m v_{ki}$, as the

weighting function, for the finite element formulation of the macro-element described earlier. It can be seen from Equ. (16) that the variation of the rotor position is represented simply by the change in the angle, θ_0 . Therefore it is very convenient to use the proposed method for dynamic analysis of PM machines without any mesh readjustment, as it will be necessary for torque prediction[2] and iron loss calculation, [e.g.,3] using the conventional FE method.

IV. APPLICATION OF M.E. TO MAGNETIC FIELD ANALYSIS OF A PERMANENT MAGNET M MACHINE

The combined finite element and analytical method described above is applied to the magnetic field analysis of a PM motor in this section. The dimensions and parameters of the machine are given as follows:

number of pole pairs	$p = 3$
Number of slots,	18
air gap length,	$g = R_1 - R_2 = 0.35$ mm
rotor outer diameter,	$R_2 = 28.4$ mm
Magnet thickness,	$l_m = R_2 - R_3 = 5.0$ mm.
Diameter of shaft,	$R_4 = 8.0$ mm.

Fig. 2 and 3 show the flux density distribution in the region of stator laminations at the rotor positions, $\theta_0 = 0^\circ$ and $\theta_0 = 30^\circ$ electrical degree, respectively. The radial components of the flux density, B_n , in air gap at $R_l = R_2 + g/2$ and in the magnet at $R_{II} = R_2 - l_m/4$ are illustrated in Figs. 4 and 5. The solid curves are computational predictions obtained from the proposed method, the points are obtained from the conventional finite element method (CFEM). Two different meshes were used in the calculations using CFEM. MESH II has a higher node density in the air gap region but the discretization of the other regions remains the same for MESH I and MESH II. The effect of the node density on the computational results obtained from CFEM can be clearly observed in Fig. 4. The computed flux density obtained from the proposed method for the region of magnet tends to be

more stable than those obtained from CFEM. As the gradient of the flux density distribution is very high in the adjacency of the magnet wall where the magnetization changes its direction, and the wave length of the flux density variation is short the numerical solution from CFEM become more sensitive to the mesh density.

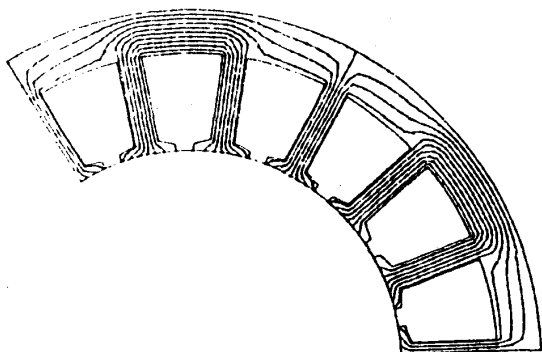


Fig. 2 Magnetic flux density distribution computed using combined finite element and analytical method for the rotor position at $\theta_0 = 0^\circ$

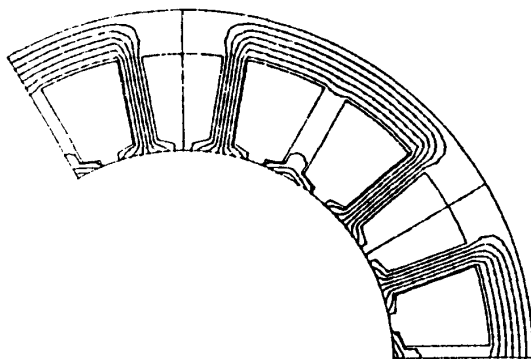


Fig. 3 Magnetic flux density distribution computed using combined finite element and analytical method for the rotor position at $\theta_0 = 30^\circ$

IV. CONCLUSIONS

An analytical solution for a macro-element that involves the region of air gap, magnet and the rotor back iron of PM electrical machines has been described in this paper. Furthermore, the solution is used to establish finite element formulation of the macro-element. The technique developed in this paper is particularly useful for field analysis of brushless dc permanent magnet machines in which there is often a low level of saturation in the rotor iron. Therefore the rotor iron can also be included in the macro-element, further simplifying the mesh generation and reducing the total number of nodes.

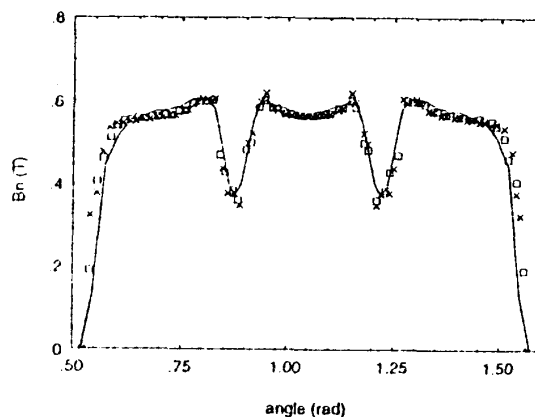


Fig. 4 Radial component of flux density in the magnet at $r = R_1$ (rotor position $\theta_0 = 0^\circ$) computed from:
 — combined finite element and analytical method
 × conventional FEM using MESH I
 o conventional FEM using MESH II

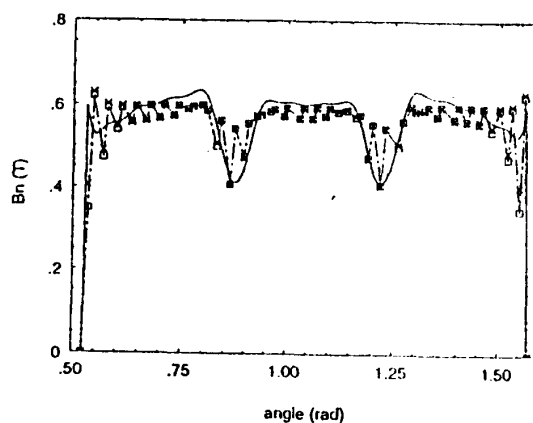


Fig. 5 Radial component of flux density in the magnet at $r = R_{II}$ (rotor position $\theta_0 = 0^\circ$) computed from:
 — combined finite element and analytical method
 × conventional FEM using MESH I
 o conventional FEM using MESH II

REFERENCE

- [1] Abdel-Razek, A. A., Coulomb, J. L., Feliachi, M. and Sabounadiere, J. C., 'The calculation of electromagnetic torque in saturated electrical machines with combined numerical and analytical solution of the field equations', *IEEE Trans. Magn.*, 17, pp 3250-3252, 1981.
- [2] Abdel-Razek, A. A., Coulomb, J. L., Feliachi, M. and Sabounadiere, J. C., 'Concept of an air-gap element for the dynamic analysis of the electromagnetic field in electrical machines', *IEEE Trans. Magn.*, 18, pp 655-659, 1982.
- [3] Liu, Z. J., Howe, D., Mellor, P. H. and Jenkins, M. K., 'Coupled thermal and electromagnetic analysis of a permanent magnet machine', *Proceeding of ICEMD'93*, vol. 1, pp 631-635, 1993.